IGF binding protein 3 exerts its ligand-independent action by antagonizing BMP in zebrafish embryos

Yingbin Zhong[1,2], Ling Lu[2], Jianfeng Zhou[2], Yun Li[2], Yunzhang Liu[2], David R. Clemmons[3] and Cunming Duan[1,*]

[1]Department of Molecular, Cellular, and Developmental Biology, University of Michigan, Ann Arbor, MI 48109, USA
[2]Key Laboratory of Marine Drugs (Ocean University of China), Chinese Ministry of Education, and School of Medicine and Pharmacy, Ocean University of China, 5 Yushan Road, Qingdao, Shandong 266003, China
[3]Department of Medicine, University of North Carolina School of Medicine, Chapel Hill, NC 27599, USA
*Author for correspondence (cduan@umich.edu)

Accepted 11 February 2011
Journal of Cell Science 124, 1925-1935

doi:10.1242/jcs.082644

Summary

IGFBP3 is a multi-functional protein that has IGF-dependent and IGF-independent actions in cultured cells. Here we show that the IGF binding domain (IBD), nuclear localization signal (NLS) and transactivation domain (TA) are conserved and functional in zebrafish Igfbp3. The in vivo roles of these domains were investigated by expression of Igfbp3 and its mutants in zebrafish embryos. Igfbp3, and its NLS and TA mutants had equally strong dorsalizing effects. Human IGFBP3 had similar dorsalizing effects in zebrafish embryos. The activities of IBD and IBD+NLS mutants were lower, but they still caused dorsalization. Thus, the IGF-independent action of Igfbp3 is not related to NLS or TA in this in vivo model. We next tested the hypothesis that Igfbp3 exerts its IGF-independent action by affecting Bmp signaling. Co-expression of Igfbp3 with Bmp2b abolished Bmp2b-induced gene expression and inhibited its ventralizing activity. Biochemical assays and in vitro experiments revealed that IGFBP3 bound BMP2 and inhibited BMP2-induced Smad signaling in cultured human cells. In vivo expression of Igfbp3 increased *chordin* expression in zebrafish embryos by alleviating the negative regulation of Bmp2. The elevated level of Chordin acted together with Igfbp3 to inhibit the actions of Bmp2 . Knockdown of *Igfbp3* enhanced the ventralized phenotype caused by *chordin* knockdown. These results suggest that Igfbp3 exerts its IGF-independent actions by antagonizing Bmp signaling and that this mechanism is conserved.

Key words: Embryos, Bone morphogenetic protein, Insulin-like growth factor, Chordin

Introduction

Genetic studies and clinical observations suggest that the insulin-like growth factor (IGF) signaling pathway has a fundamental role in regulating animal growth and development, as well as in maintaining adult homeostasis (Clemmons, 2007; Duan and Xu, 2005; Firth and Baxter, 2002). Most, if not all, IGFs in extracellular fluid are present in complexes with specific, high-affinity IGF binding proteins (IGFBPs). In the bloodstream, the majority of circulating IGFs are in a ternary complex with IGFBP3 and a protein termed acid-labile subunit (ALS) (Firth and Baxter, 2002; Yamada and Lee, 2009). This ternary complex not only serves as a reservoir for IGF release, but also greatly increases the half-life of IGFs. In addition, the IGF–IGFBP complexes in the circulation and in tissues help to prevent potential cross binding of IGFs to the insulin receptor. Therefore, IGFBP3 functions as a carrier protein and regulates circulating IGF turnover, transport, and distribution.

IGFBP3 is a member of the IGFBP gene family. Similarly to other IGFBPs, IGFBP3 is comprised of three recognizable domains of similar size (~80 residues): an N-terminal domain, typically with 12 conserved cysteine residues, a C-terminal domain with six conserved cysteine residues, and a central L-domain that is thought to act as a hinge between the N- and C-domains (Firth and Baxter, 2002; Yamada and Lee, 2009). The N- and C-domains are required for high-affinity ligand binding and are highly conserved across species (Duan and Xu, 2005). In addition to its role as the major IGF carrier protein in the circulation, IGFBP3 has also been shown to inhibit and/or potentiate the actions of IGF in a wide variety of cultured human and rodent cells. Furthermore, IGFBP3 has been shown to possess distinct biological effects independently of IGF (Firth and Baxter, 2002; Jogie-Brahim et al., 2009; Yamada and Lee, 2009). There is general agreement that the IGF–IGF-1R-independent actions of IGFBP3 might contribute to the pathophysiology of a number of human diseases, including cancer and diabetes, although the actual role of IGFBP3 is still unclear (Firth and Baxter, 2002; Jogie-Brahim et al., 2009; Yamada and Lee, 2009). Recent studies have implicated the interaction of IGFBP3 with a variety of proteins or signaling cascades that are crucial to cell proliferation and/or apoptosis (Firth and Baxter, 2002; Jogie-Brahim et al., 2009; Yamada and Lee, 2009).

Despite these advances, many important questions remain. IGFBP3 has been shown to exhibit ligand-dependent, as well as ligand-independent, actions in cultured mammalian cells. However, its in vivo modes of action and the underlying mechanisms are poorly understood. Mammalian IGFBP3 has a functional NLS and can be found in the nucleus of cultured tumor cells (Firth and Baxter, 2002; Jogie-Brahim et al., 2009), but the functional significance of this NLS in mediating the ligand-independent actions of IGFBP3 is also unclear and whether the NLS of IGFBP3 has a role in vivo is unknown. Likewise, the mammalian IGFBP3 N-domain contains a functional transactivation domain (Zhao et al., 2006). It is not clear whether this activity is conserved or whether it has any biological significance in vivo.

Most research on the developmental role of IGFs and IGFBPs has relied on rodent models, and attempts to elucidate the molecular

and cellular basis of IGFBP have been hampered by the inaccessibility of the mammalian fetus enclosed in the uterus and the greater redundancy of mammalian systems. We have shown that zebrafish Igfbp3 has an important role in the formation and differentiation of the pharyngeal skeleton and inner ear (Li et al., 2005). The objectives of this study were to determine: (1) whether the IGF binding domain (IBD), nuclear localization signal (NLS), and transactivation domain (TA) are conserved in zebrafish Igfbp3; (2) whether Igfbp3 can use any of these domains to exert ligand-dependent and/or ligand-independent actions in an in vivo setting; and (3) the molecular mechanisms underlying its IGF-independent actions.

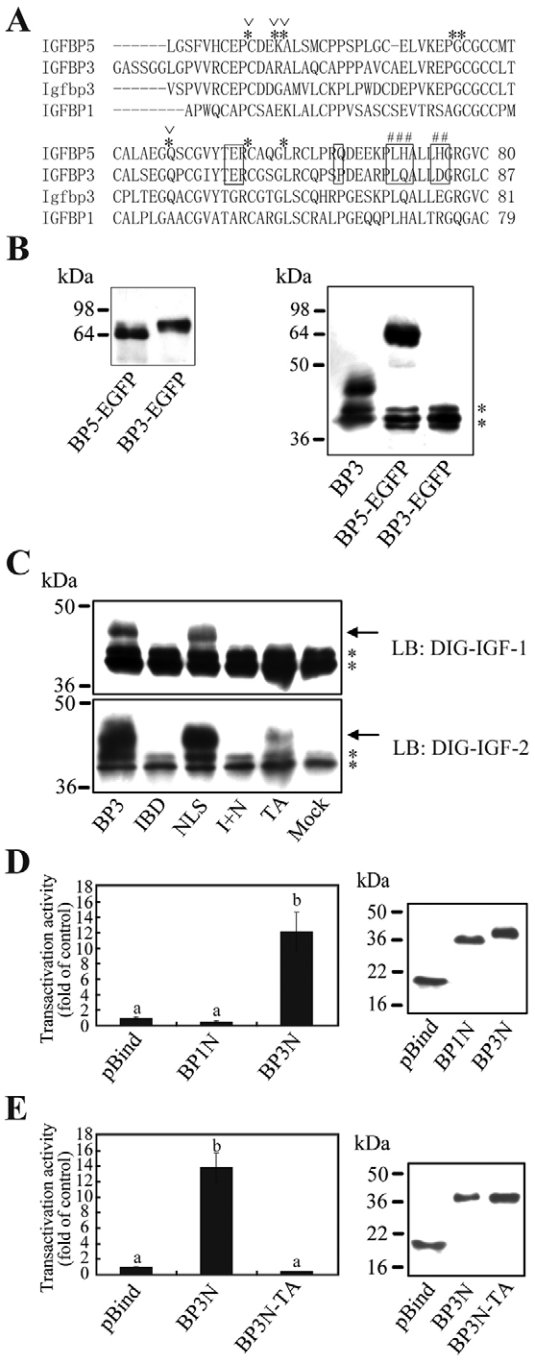

Results

The NLS, IBD and TA domains are conserved and functional in zebrafish Igfbp3

Human IGFBP3 binds IGFs primarily using its high-affinity binding site located in the N-domain, although its C-domain also has a role (Buckway et al., 2001; Hong et al., 2002; Imai et al., 2000). According to Imai and colleagues (Imai et al., 2000), R69, P70, L71, L74 and L75 are particularly crucial for its IGF binding. Sequence analysis indicates that these residues are all conserved in zebrafish Igfbp3 (Fig. 1A). To ascertain that zebrafish Igfbp3 is a functional IGFBP, we constructed an expression plasmid by subcloning the zebrafish Igfbp3 ORF into the pCS2+EGFP plasmid. A human IGFBP5 pCS2+EGFP plasmid was used as a positive control. After these mutants were introduced into HEK293T cells by transient transfection, conditioned medium was prepared and analyzed. Western immunoblotting results showed the successful expression and secretion of Igfbp3–EGFP and IGFBP5–EGFP fusion proteins (Fig. 1B, left panel). Unexpectedly, ligand blotting analysis showed that human IGFBP5–EGFP but not zebrafish Igfbp3–EGFP was capable of IGF binding (Fig. 1B, right panel). We speculated that tagging of EGFP to the zebrafish Igfbp3 might disrupt its ligand-binding property. To test this idea, we constructed a new expression plasmid by subcloning the zebrafish Igfbp3 ORF into the pCS2+ vector. When the plasmid was introduced in HEK293T cells, a novel IGFBP of approximately 45 kDa was detected in the conditioned medium (Fig. 1B, right), suggesting that the zebrafish Igfbp3 ORF indeed encodes a functional IGFBP. Zebrafish Igfbp3 was able to bind both IGF-1 and IGF-2 (Fig. 1C). To determine whether the conserved IGF binding domain (IBD) in

Fig. 1. The IGF binding domain (IBD) and transactivation (TA) domain are conserved and functional in zebrafish Igfbp3. (**A**) Sequence alignment of the N-domain of human IGFBP5, IGFBP3, IGFBP1 and zebrafish Igfbp3. Open boxes indicate residues known to be crucial for IGF binding in human IGFBP5 and IGFBP3. # marks the five residues altered by site-directed mutagenesis in the IBD mutant. Asterisks indicate residues known to be important for the TA activity in human IGFBP5, and the four residues altered by site-directed mutagenesis in the TA dead mutant are indicated by carets. (**B**) Western immunoblotting (left) and ligand blotting (right) analysis of human IGFBP5–EGFP (BP5-EGFP), zebrafish Igfbp3–EGFP (BP3-EGFP) and zebrafish Igfbp3 (BP3) using anti-GFP antibody and DIG-labeled human IGF-1, respectively. Asterisks denote endogenous IGFBPs, serving as internal controls. (**C**) Ligand-blotting analysis of culture medium conditioned by HEK293T cells transfected with zebrafish Igfbp3 (BP3), its IBD, NLS, IBD+NLS (I+N), TA dead (TA) mutant or empty vector (Mock). Arrows denote zebrafish Igfbp3 and its mutant proteins. Asterisks denote the endogenous IGFBPs, serving as internal controls. Upper panel shows results using DIG-labeled human IGF-1 and lower panel using DIG-labeled human IGF-2. (**D**) Zebrafish Igfbp3 N-domain has transactivation activity. The N-domain of zebrafish Igfbp3 (BP3N) and human IGFBP1 (BP1N) were fused to Gal4 DNA-binding domain and transfected into HEK293T cells together with a Gal4 reporter plasmid. The transactivation activity is expressed as fold increase over the pBind control group. Values are expressed as means ± s.d., n=3. Groups with different letters are significantly different from each other (P<0.05). The expression levels of these fusion proteins were analyzed by western immunoblotting using an anti-GAL4 antibody and shown in the right panel. (**E**) The TA-dead mutant (BP3N-TA) has no transactivation activity. Values are expressed as fold increase over the pBind control group. Values are means ± s.d., n=3. Groups with different letters are significantly different from each other (P<0.05). The expression levels of these mutant fusion proteins are shown in the right panel.

zebrafish Igfbp3 is responsible for its IGF binding, and to generate an IBD mutant for subsequent in vivo functional analysis, we generated a zebrafish Igfbp3 IBD mutant by changing K70, P71, L72, L75, and L76 of zebrafish Igfbp3 to N70, Q71, Q72, Q75 and Q76, respectively. As shown in Fig. 1C, this mutant did not bind to IGF-1 or IGF-2.

Previous studies suggest that mammalian IGFBP3 is not only secreted but is also present in the nucleus (Firth and Baxter, 2002), and its N-domain has transactivation activity (Xu et al., 2004; Zhao et al., 2006). To determine whether this activity is conserved, the zebrafish Igfbp3 N-domain (amino acids 1–81) was fused to the Gal4 DNA-binding domain (Gal4DBD), and the activity was measured. As shown in Fig. 1D, the zebrafish Igfbp3 N-domain caused a 12.18±2.53-fold increase in GAL4-dependent transactivation (n=3, P<0.001). In comparison, the IGFBP-1 N-domain had no significant activity. Western immunoblot analysis revealed that expression levels of these fusion proteins were similar (Fig. 1D). We next compared the sequence of the zebrafish Igfbp3 N-domain with that of human IGFBP5 N-domain, whose transactivation domain (TA) has been extensively characterized (Xu et al., 2004; Zhao et al., 2006). Among the eight residues in the human IGFBP5 N-domain that are known to be crucial for its transactivation ability (Zhao et al., 2006), six (E8, D11, D12, E31, P32 and E44) are conserved in zebrafish Igfbp3 (Fig. 1A). Importantly, these six residues are not conserved in human IGFBP-1, which has no transactivation activity (Xu et al., 2004) (also see Fig. 1D). We generated a TA-dead mutant for subsequent functional analyses by mutating E8, D11, D12 and E44 of zebrafish Igfbp3 into the corresponding residues in human IGFBP1 (E8A, D11S, D12A, E44L). As shown in Fig. 1E, the TA-dead mutant (BP3N-TA) had essentially no transactivation activity. The expression levels of the fusion protein were similar (Fig. 1E, right), thus excluding the possibility that the difference was due to different levels of protein expression and/or degradation. Of note, the TA mutant was capable of IGF binding, although the binding appeared to be somewhat reduced (Fig. 1C).

Radulescu (Radulescu, 1995) recognized that several basic residues in the human IGFBP3 C-domain resembled a bipartite nuclear localization signal (NLS). Schedlich and co-workers (Schedlich et al., 1998) provided experimental evidence showing that mutation of 228-KGRKR-232 into MDGEA abolished the nuclear transport of human IGFBP3. This bipartite NLS is well conserved in zebrafish Igfbp3 (Fig. 2A). When cells were transfected with zebrafish Igfbp3–EGFP, the signal was seen exclusively in the nucleus, often as a number of dots or speckles within the nucleus (Fig. 2B). In comparison, the zebrafish Igfbp1a–EGFP signal was only detected in the cytoplasm (Fig. 2B). We next engineered a NLS mutant by changing four basic residues (236-KGRK-239) in the NLS of zebrafish Igfbp3 into the corresponding sequence of zebrafish Igfbp1a, LDGQ (Maures and Duan, 2002) (Fig. 2A). This NLS mutant showed no nuclear localization (Fig. 2B), but had normal IGF binding (Fig. 1C). We also engineered and tested an IBD and NLS double mutant (IBD+NLS). As shown in Fig. 1C and Fig. 2B, the IBD+NLS double mutant had impaired IGF binding and nuclear localization. The TA mutant, however, had normal nuclear localization (Fig. 2B).

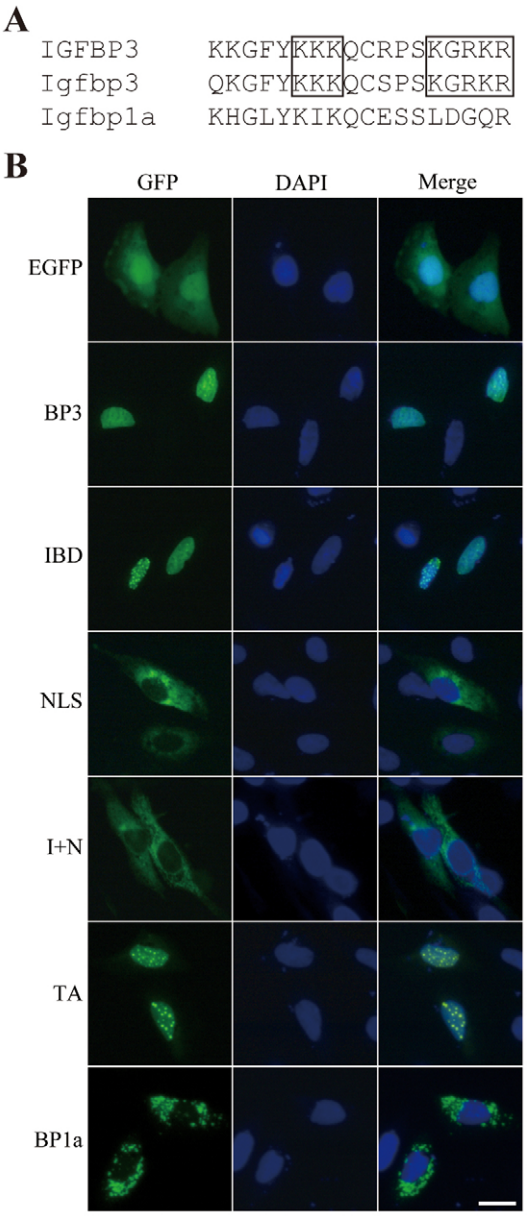

Fig. 2. Subcellular localization of zebrafish Igfbp3 and its various mutants. (**A**) Sequence alignment of the nuclear localization signal (NLS) motif in human IGFBP3 and zebrafish Igfbp3 and the corresponding region of zebrafish Igfbp1a. The conserved crucial residues are boxed. (**B**) U2OS cells were transfected with zebrafish Igfbp3–EGFP (BP3), its IBD mutant, NLS mutant, IBD+NLS double mutant (I+N), or TA mutant expression plasmid. Zebrafish Igfbp1a-EGFP (BP1a) and pC2+EGFP were used as negative controls. The EGFP signal was visualized (left panel) 24 hours after transfection. Corresponding DAPI staining is shown in the middle column and merged views in the right column. Scale bar: 25 μm.

Zebrafish Igfbp3 exerts ligand-dependent and ligand-independent effects in vivo

To determine the functional roles of its conserved IBD, TA and NLS in vivo, capped mRNAs encoding zebrafish Igfbp3 and its various mutants were introduced into zebrafish embryos by microinjection. As shown in Fig. 3A, forced expression of Igfbp3 caused shortened tail or a loss of tail and truncated body plan. Based on the severity of the phenotypes, we grouped them into three categories: weak, medium and severe (Fig. 3A). As shown in Fig. 3B, forced expression of Igfbp3 resulted in more than 40% abnormal embryos, whereas control embryos injected with *egfp*

mRNA alone were indistinguishable from intact embryos. In the group injected with mRNA encoding Igfbp3 with a mutated IBD (i.e. the IBD mutant), only about 20% of the embryos showed weak or medium phenotypes. The results in the IBD+NLS double mutant group were very similar to those of the IBD group (Fig. 3B). The results of the NLS mutant and TA mutant group were similar to those of the wild-type Igfbp3 group. As mentioned above, tagging EGFP to zebrafish Igfbp3 reduced its IGF binding ability (Fig. 1B). Taking advantage of this finding, we injected mRNA encoding Igfbp3–EGFP into zebrafish embryos as an independent way to examine the IGF-binding-independent action. As shown in Fig. 3C, more than 40% of the embryos in this group showed an abnormal phenotype, whereas all embryos in the control EGFP group were normal (Fig. 3C).

To determine whether the observed phenotypes were due to changes in the dorsal–ventral axis, we performed in situ hybridization using a number of dorsal–ventral axis marker genes. *floating head* (*flh*) expression marks the dorsal axial mesoderm at the stages of shield and 60% epiboly (Miller-Bertoglio et al., 1997; Talbot et al., 1995). *even-skipped-1* (*eve1*) and *ventral edema* (*ved*) (Joly et al., 1993; Shimizu et al., 2002) are expressed in the ventral non-axial mesoderm. *T-box 24* (*tbx24*) is expressed in the paraxial mesoderm at the stage of 80% epiboly (Nikaido et al., 2002). Expression of zebrafish Igfbp3 or its IBD mutant markedly increased the expression domains of *flh* (Fig. 3Dc,d). By contrast, the expression domains of *eve1* and *ved* were reduced in embryos injected with mRNA encoding Igfbp3 or its IBD mutant (Fig. 3Dg,h,k,l and k′,l′). Forced expression of Igfbp3 or its IBD mutant also squeezed or pushed the *tbx24* expression domains to the lateral sides, probably as a result of expansion of the dorsal organizer (Fig. 3Do,p,o′,p′). These findings suggest that Igfbp3 and its IBD have dorsalizing effects in zebrafish embryos.

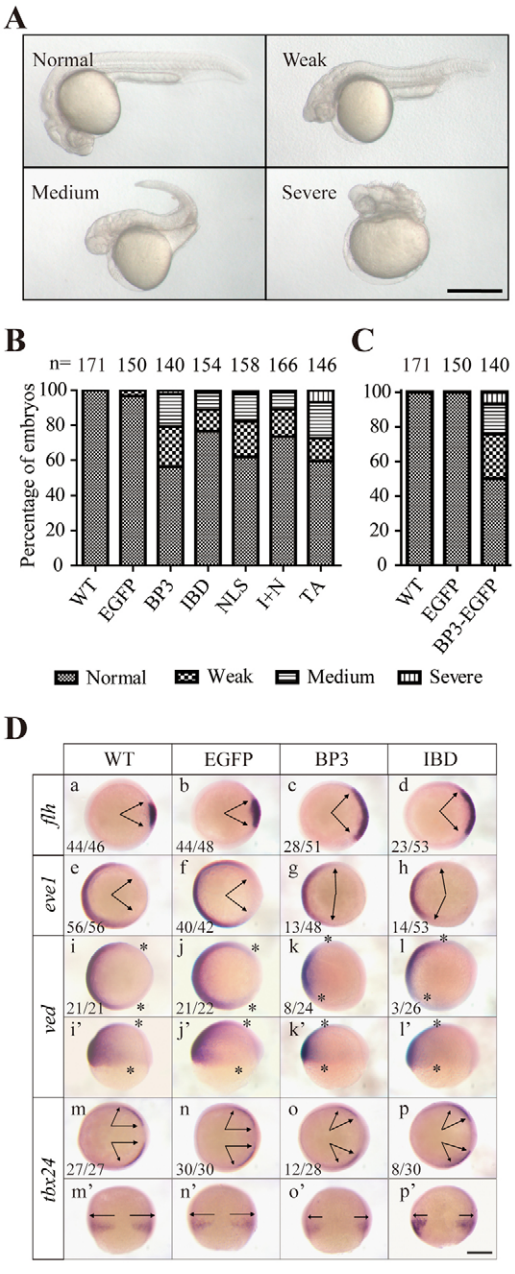

Igfbp3 exerts its IGF-independent action by antagonizing Bmp2 signaling in vivo

The dorsalization of embryos caused by Igfbp3 resemble the phenotypes of *swirl* and *somitabun*, two zebrafish genetic mutant lines caused by the loss of *bmp2b* and its signaling transducer *smad5*, respectively (Hild et al., 1999; Kishimoto et al., 1997). We postulated that Igfbp3 might exert its IGF-independent action by affecting BMP signaling. To test this hypothesis, co-expression experiments were performed. As reported (Kishimoto et al., 1997), injection of *bmp2b* mRNA had ventralizing effects in zebrafish embryos (Fig. 4Av1–v4). Co-injection of zebrafish *igfbp3* mRNA with *bmp2b* mRNA markedly reduced the ventralizing effect of Bmp2b (Fig. 4A,B). IBD had similar antagonizing effects (Fig. 4A,B).

We next examined the interaction between Igfbp3 and Bmp2b in the formation of the dorsal–ventral axis. As shown in Fig. 4C, forced expression of Bmp2b markedly reduced the expression domains of *flh*, a dorsal marker gene, and co-expression of either zebrafish Igfbp3 or its IBD mutant abolished this Bmp2b-related reduction in expression (Fig. 4Cc,d,g,h; and Fig. 4D). Forced expression of Bmp2b markedly increased the expression domains

Fig. 3. Igfbp3 exerts both IGF-dependent and IGF-independent actions in zebrafish embryos. (**A**) Classification of phenotypes caused by forced expression of zebrafish Igfbp3. 1- to 2-cell embryos were injected with zebrafish *igfbp3* mRNA and raised to 24 h.p.f. Lateral views are shown. Scale bar: 0.5 mm. (**B**) EGFP, zebrafish Igfbp3, IBD mutant, NLS mutant, IBD+NLS double mutant (I+N), or TA mutant mRNA was injected into 1- to 2-cell-stage embryos. The embryos were raised to 24 h.p.f. and their phenotypes were scored based on the categories shown in A. The percentage of embryos in each category is shown. The results shown are from three independent injection experiments and the total embryo number in each group is shown on the top. (**C**) 24 h.p.f. wild-type embryos (WT), or embryos injected with *egfp* mRNA (EGFP) or zebrafish *igfbp3-egfp* mRNA (BP3-EGFP) were scored based on the categories shown in A and the percentage of embryos in each category is shown. (**D**) Wild-type embryos (WT) or embryos injected with mRNA encoding EGFP (EGFP), zebrafish Igfbp3 (BP3) or IBD mutant (IBD) were analyzed by whole-mount in situ hybridization using the indicated probes. The frequency of embryos with the indicated expression patterns is shown in the bottom left corner of each panel. Panels a–p are animal pole view with dorsal to the right; panels i′–l′ are lateral view with animal pore up and dorsal to the right; m′–p′ are dorsal view with animal pore up. Arrows indicate the width of the expression domain. Asterisks indicate the edges of *ved* expression domain. Panels a–l and i′–l′, embryos at 60% epiboly; m–p and m′–p′, 80% epiboly. Scale bar: 0.25 mm.

of *eve1* mRNA (Fig. 4Cf and Fig. 4E). Co-expression of zebrafish Igfbp3 or its IBD mutant with Bmp2b, restored the expression of *eve1* to control levels (Fig. 4Cg,h, Fig. 4E). Similar results were obtained with *ved* mRNA (Fig. 4Cj–l,j′–l′; Fig. 4F). Forced expression of Bmp2b also caused expression domains of *tbx24* to converge in the middle point as a result of the reduction of the dorsal organizer size (Fig. 4Cn,n′; Fig. 4G). Co-expression of Bmp2b with Igfbp3 or its IBD mutant restored the *tbx24* expression domains to the wild type and EGFP control levels (Fig. 4Co,p,o′,p′; Fig. 4G).

To provide further evidence that Igfbp3 antagonizes Bmp2 signaling in zebrafish embryos, we examined the effect of Igfbp3 on Bmp2b-induced *tp63* gene expression using whole-mount in situ hybridization and real-time quantitative RT-PCR (qRT-PCR). *tp63* is a direct transcriptional target of Bmp signaling in zebrafish (Bakkers et al., 2002). Injection of *bmp2b* mRNA alone resulted in a marked expansion in the *tp63* mRNA expression domains (Fig. 5A,B). Injection of mRNA encoding the Igfbp3 IBD mutant, however, caused a major reduction in *tp63* mRNA expression domains. Most embryos co-injected with mRNA encoding Bmp2b and the IBD mutant had an expression pattern that was similar to the *egfp* mRNA control embryos (Fig. 5A,B). The qRT-PCR results are shown in Fig. 5C. Forced expression of Bmp2b resulted in a highly significant tenfold increase in *tp63* mRNA levels. Co-expression of Igfbp3 or its IBD mutant significantly inhibited the Bmp2b-induced increase in *tp63* mRNA expression. Expression of Igfbp3 alone resulted in a significant decrease in *tp63* mRNA levels (Fig. 5C). These results suggest that Igfbp3 antagonizes Bmp2 signaling in vivo and that this action of Igfbp3 is largely independent of IGF binding.

IGFBP3 binds BMP2 and inhibits signaling and also upregulates chordin gene expression

Many BMP antagonists, such as Chordin, Noggin and Follistatin, inhibit BMP signaling by direct binding to BMP ligand (Iemura et al., 1998; Piccolo et al., 1996; Zimmerman et al., 1996). We carried out western ligand blotting assays to test whether IGFBP3 can interact with BMP2 physically. As shown in Fig. 6A, DIG-labeled BMP2 bound Noggin, which is well-established to bind and antagonize BMP. Likewise, DIG–BMP2 bound IGFBP3, albeit at a higher concentration. In comparison, DIG–BMP2 did not bind to IGFBP1 and IGFBP6, two closely related proteins, but DIG-labeled IGF-1 or IGF-2 was able to bind all three IGFBPs, but not Noggin (supplementary material Fig. S1). In the absence of zebrafish

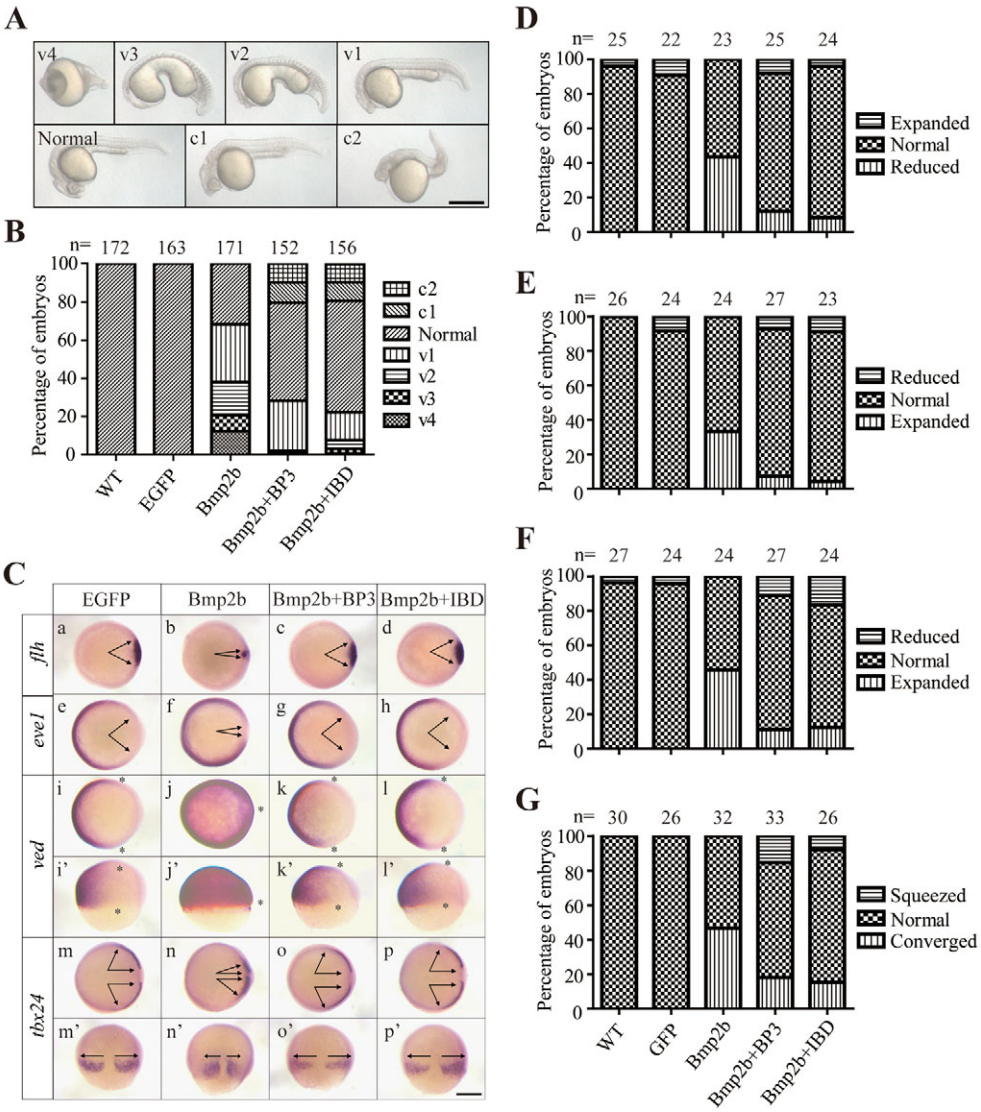

Fig. 4. Igfbp3 antagonizes Bmp2b action in zebrafish embryos via an IGF binding independent mechanism. (**A**) Classification of phenotypes caused by forced expression of zebrafish Bmp2b with zebrafish Igfbp3. Lateral views of 24 h.p.f. embryos are shown with dorsal up. Ventralized embryos are classified into four levels as indicated in v1–v4. Dorsalized embryos are classified into two levels as shown in c1 and c2. Scale bar: 0.5 mm. (**B**) embryos injected with the indicated mRNAs were raised to 24 h.p.f. and their phenotypes were scored based on the categories shown in A. Percentage of embryos in each category is shown. The results are from three independent experiments and the total embryo number is given on the top. (**C**) Embryos injected with the indicated mRNAs were analyzed by whole mount in situ hybridization using the indicated probes. Panels a–p are animal pole view with dorsal to the right; panels i′–l′ are lateral view with animal pore up and dorsal to the right; m′–p′ are dorsal view with animal pole up. Arrows indicate the width of the expression domain; asterisks indicate the edges of the *ved* mRNA expression domain. Panels a–l and i′–l′, embryos at 60% epiboly; m–p and m′–p′, 80% epiboly. Scale bar: 0.25 mm. Percentage of embryos in each category was calculated and shown in **D** (*flh*), **E** (*eve1*), **F** (*ved*) and **G** (*tbx24*). The total embryo number is shown on the top of each bar.

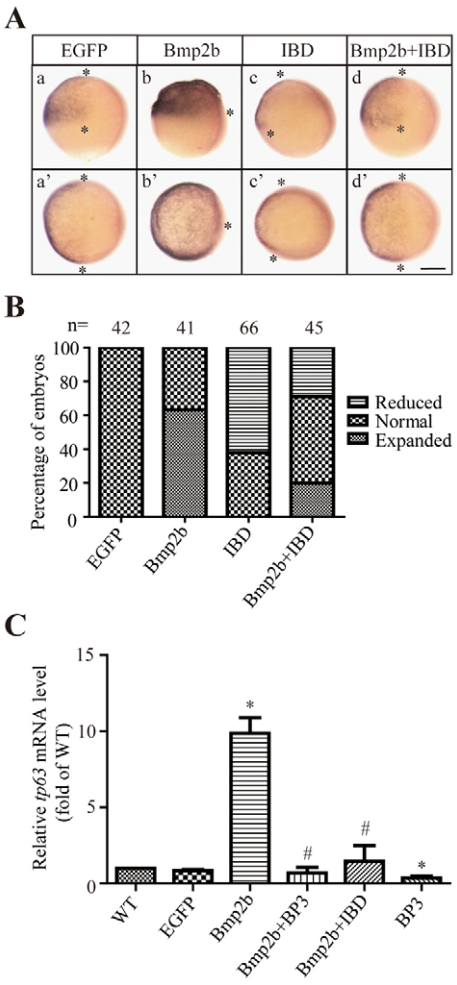

Fig. 5. Expression of zebrafish Igfbp3 abolishes Bmp2b-induced target gene expression in zebrafish embryos. (**A**) Whole mount in situ analysis results of *tp63* mRNA expression in embryos injected with the indicated mRNA. a–d, lateral views with animal pore up and dorsal to the right; a′–d′, animal pole views with dorsal to the right. Asterisks indicate the edges of the *tp63* mRNA expression domain. Embryos are at 80% epiboly. Scale bar: 0.25 mm. (**B**) Percentage of embryos in each category. The total embryo number is shown on the top. (**C**) qRT-PCR results. Embryos were injected with the indicated mRNA and raised to the 60% epiboly stage. The *tp63* mRNA levels were measured by qRT-PCR and normalized to *β-actin* mRNA. The data are expressed as fold increase over the wild-type (WT) group. Values are expressed as means ± s.d., n=3. *P<0.01 vs WT and GFP group; $^{\#}P$<0.01 vs the Bmp2b group.

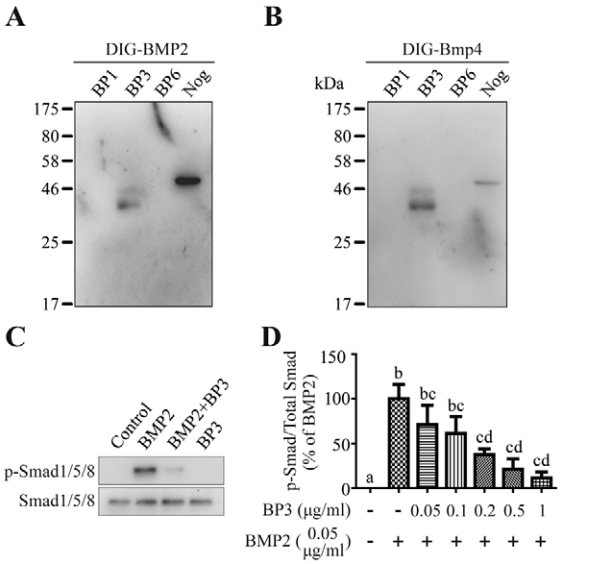

Fig. 6. IGFBP3 binds to BMP2 and inhibits BMP2-induced Smad phosphorylation. (**A**) Ligand-blotting analysis of purified IGFBP1 (BP1), IGFBP3 (BP3), IGFBP6 (BP6) and Noggin (Nog) proteins using DIG-labeled BMP2 as ligand. Similar results were obtained from four experiments. (**B**) Ligand-blotting analysis using DIG-labeled zebrafish Bmp4 as ligand. Similar results were obtained from three other experiments. (**C**) IGFBP3 inhibits BMP2 signaling in vitro. 0.05 μg/ml BMP2 premixed with or without 0.5 μg/ml IGFBP3 was added to cultured U2OS cells. 3 hours later, cells were lyzed and subjected to western immunoblotting analysis using antibodies against total or phosphorylated Smad1/5/8. A representative gel is shown. (**D**) Dose-dependent effect of IGFBP3 in inhibiting BMP2 signaling. Values are expressed as means ± s.d., n=3. Groups with different letters are significantly different from each other (P<0.05).

Bmp2b protein, we tested whether IGFBP3 can bind to zebrafish Bmp4, which is structurally closely related to Bmp2. As shown in Fig. 6B, DIG-labeled zebrafish Bmp4 also bound IGFBP3 and Noggin, but not IGFBP1 and IGFBP6. These results suggest that IGFBP3 can directly bind BMP2 and BMP4. The effect of this binding on BMP2 signaling was determined by measuring BMP2-induced phosphorylation of the Smad1, Smad5 and Smad8 complex (Samd1/5/8) in cultured U2OS cells. BMP2 strongly induced Smad phosphorylation in this in vitro model (Fig. 6C). Co-incubation with IGFBP3 inhibited BMP2-induced Smad phosphorylation in a dose-dependent manner, whereas IGFBP3 alone had little effect (Fig. 6C,D). These results suggest that IGFBP3 can bind to and inhibit BMP2 signaling.

It is known that the expression of the *chordin* gene, which causes dorsalization, is under the negative regulation of Bmp2 (Zakin and De Robertis, 2010). If Igfbp3 indeed bound to and inhibited Bmp2b signaling in vivo, overexpression of Igfbp3 should remove this negative regulation and increase *chordin* expression in vivo. To test this idea, we analyzed *chordin* mRNA expression in embryos injected with *igfbp3* mRNA and mRNA encoding the IBD mutant. Many of these injected embryos had expanded the *chordin* mRNA expression domains (Fig. 7A,B). Co-injection experiments with *bmp2b* mRNA resulted in a marked reduction in the *chordin* mRNA expression domain (Fig. 7C,D). This effect of Bmp2b was alleviated by the co-injection of mRNA encoding either Igfbp3 or its IBD mutant (Fig. 7C,D). In good agreement with the in situ hybridization results, qRT-PCR analysis also showed that forced expression of Igfbp3 significantly increased *chordin* mRNA levels (Fig. 7E). By contrast, expression of Bmp2b resulted in a highly significant decrease in *chordin* mRNA levels. Co-expression of either Igfbp3 or its IBD mutant with Bmp2b reversed the inhibitory effect of Bmp2b on *chordin* expression (Fig. 7E). These results suggest that Igfbp3 inhibits Bmp2 signaling in vivo.

Chordin regulates dorsal development, and overexpression of Chordin can dorsalize zebrafish embryos (Hammerschmidt et al., 1996; Miller-Bertoglio et al., 1997; Piccolo et al., 1996). To test

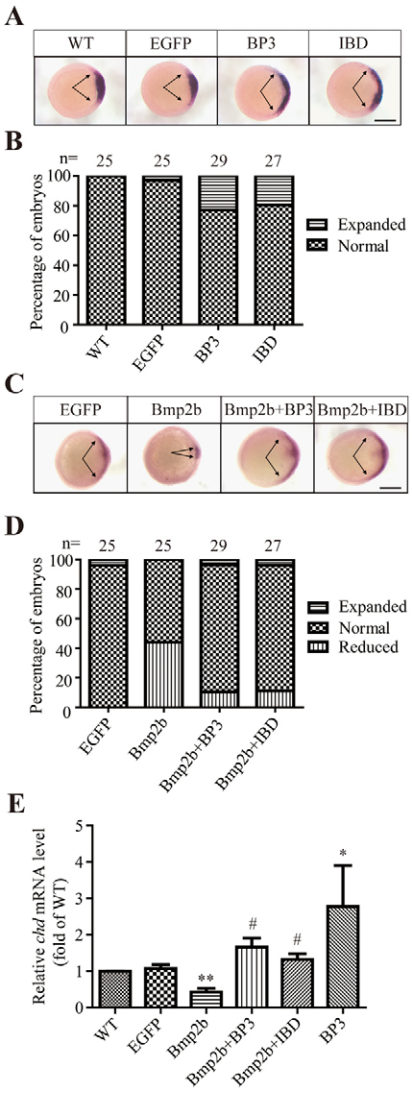

Fig. 7. Igfbp3 upregulates *chordin* gene expression by alleviating the negative regulation of Bmp2. Whole-mount in situ analysis results of *chordin* mRNA expression in wild-type embryos or embryos injected with the indicated mRNA at shield stage (**A**) or 60% epiboly (**C**). Animal pole views are shown with dorsal to the right. Arrows indicate the width of expression domains. Scale bar: 0.25 mm. (**B**,**D**) Percentage of embryos in each category shown in A or C, respectively. Total embryo number is on the top. (**E**) qRT-PCR analysis results. *chordin* mRNA levels of the indicated group were measured by qRT-PCR and normalized by β-actin mRNA level. The results are expressed as fold increase over the wild-type (WT) group. Values shown are means ± s.d., n=3. *P<0.05 and **P<0.01 vs WT and GFP group; $^{\#}P$<0.01 vs the Bmp2b group.

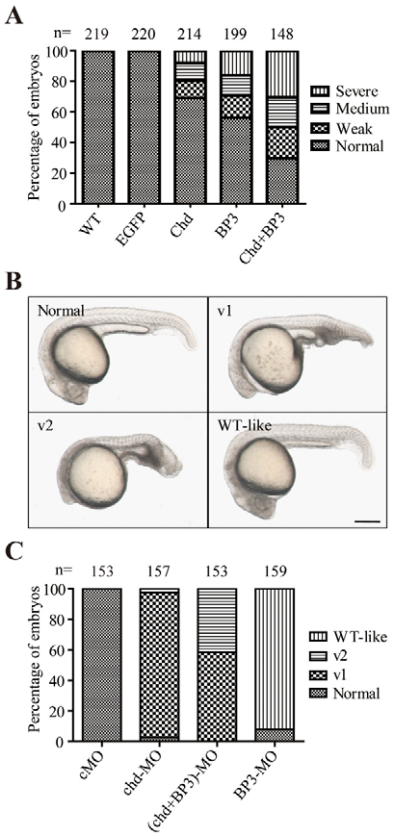

Fig. 8. Igfbp3 acts in concert with Chordin to antagonize Bmp2 actions in zebrafish embryos. (**A**) Igfbp3 and Chordin have additive dorsalizing effects. Zebrafish embryos were injected with the indicated mRNA, raised to 24 h.p.f., and analyzed according to the phenotype categories shown in Fig. 3A. The results shown are from three independent experiments with the total embryo number shown on the top. (**B**,**C**) Igfbp3 functions redundantly to Chordin in antagonizing Bmp action. 1- to 2-cell-stage zebrafish embryos were injected with the indicated MOs, raised to 24 h.p.f., and analyzed according to the phenotype categories shown in B. The frequency of each group was shown in C, which was tabulated from three independent experiments with the total embryo number shown on the top. Scare bar: 0.25 mm.

whether Igfbp3 and Chordin act additively or synergistically in inhibiting Bmp2 signaling, we co-injected *chordin* mRNA and *igfbp3* mRNA into zebrafish embryos. Igfbp3 and Chordin had additive dorsalizing effects in zebrafish embryos (Fig. 8A). To investigate the physiological role of Igfbp3 and its relationship with Chordin, we performed experiments to knock down Igfbp3 and Chordin individually and in combination, using validated morpholino-modified oligonucleotides (MOs). Knockdown of Igfbp3 alone caused defective pharyngeal arches, but it did not alter dorsal–ventral patterning (Fig. 8B,C, WT-like phenotype). Injection of Chordin MO alone resulted in a modest degree of ventralization in over 90% of the embryos (Fig. 8B,C). Embryos co-injected with *chordin* MO and *igfbp3* MO showed a more severe ventralized phenotype, with greatly reduced head, expanded hematopoietic tissues and an enlarged tail (Fig. 8B,C; supplementary material Fig. S2). These new results indicate that Igfbp3 acts in a redundant manner with Chordin to antagonize Bmp2 action in zebrafish embryos.

The BMP-antagonist action of IGFBP3 is evolutionarily conserved

To determine whether the BMP-antagonizing action is conserved, we injected mRNA encoding human IGFBP3 and its IBD mutant into zebrafish embryos. Similarly to the use of zebrafish Igfbp3, forced expression of human IGFBP3 or its IBD mutant resulted

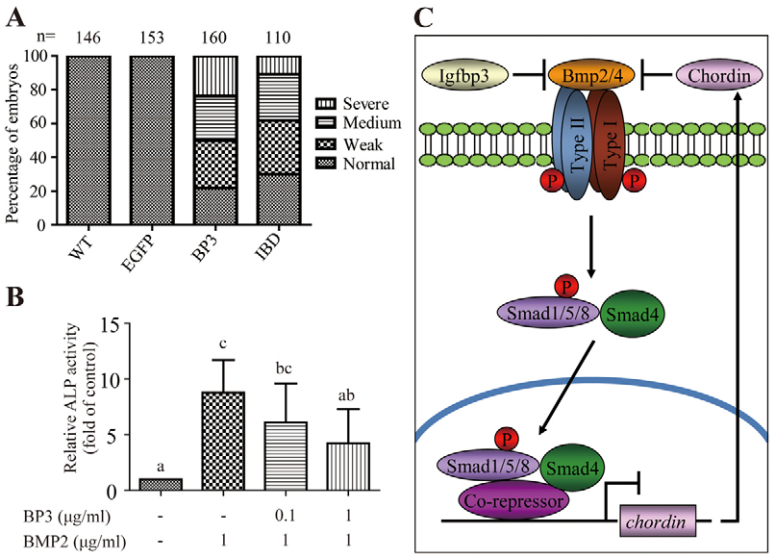

Fig. 9. The BMP-antagonizing action of IGFBP3 is evolutionarily conserved. (**A**) 1- to 2-cell-stage embryos were injected with mRNA encoding human IGFBP3 (BP3) or its IBD mutant (IBD). The injected embryos were raised to 24 h.p.f. and analyzed according to the phenotype categories shown in Fig. 3A. The results shown are from three independent experiments with the total embryo number shown on the top. (**B**) Human IGFBP3 inhibits BMP2-induced cell differentiation. 10T1/2 cells were treated with or without human IGFBP3 (BP3). 48 hours later, cells were changed into serum-containing medium supplemented with human BMP2 (1 μg/ml). Four days later, cells were harvested and subjected to ALP activity assay. The ALP activity was normalized by total protein levels and expressed as fold over the control. Values are means ± s.d., n=6. Groups with different letters are significantly different from each other (P<0.05). (**C**) A proposed model on the involvement of Igfbp3 in the Bmp signaling pathway in zebrafish embryos. Igfbp3 binds to Bmp2–Bmp4 (Bmp2/4) and inhibits its binding to its receptor and thereby Smad signaling. The reduced Bmp2/4 signaling leads to an increase in *chordin* gene expression as a result of alleviation of the negative regulation of Bmp2/4. The increased Chordin acts together with Igfbp3 to further antagonize Bmp2/4 activity, which in turn, results in dorsalized embryos.

in dorsalized zebrafish embryos in approximately 80% and 70% of the injected embryos, respectively (Fig. 9A). To further address this issue, we examined the effect of IGFBP3 on BMP2-induced differentiation of mouse 10T1/2 cells. As reported by Katagiri and colleagues (Katagiri et al., 1990), when human BMP2 was added to cultured 10T1/2 cells, it caused a significant eightfold increase in ALP activity (Fig. 9B). Addition of human IGFBP3 inhibited the BMP2-induced increase in ALP activity in a concentration-dependent manner (Fig. 9B). These findings suggest that the BMP2-antagonizing action of IGFBP3 is evolutionarily conserved.

Discussion

In this study, we show that Igfbp3 acts in both IGF-binding-dependent and -independent manners in zebrafish embryos and the IBD, NLS and TA domains are all conserved and functional in zebrafish Igfbp3. Taking advantage of the zebrafish model, we examined the in vivo roles of these domains using a transgenic approach. The results suggest that the IGF-independent action of zebrafish Igfbp3 is not related to its nuclear localization or transactivation activity. Our genetic and biochemical experiments reveal that Igfbp3 exerts its IGF-independent actions by inhibiting Bmp2 signaling, and this mechanism is evolutionarily conserved.

In a previous study, we showed that targeted knockdown of the zebrafish *igfbp3* gene resulted in defects in the development of pharyngeal cartilage and the inner ear (Li et al., 2005). These actions of Igfbp3 are probably IGF-dependent because targeted knockdown or dominant-negative inhibition of the IGF-1 receptor also resulted in defects in pharyngeal cartilage and the inner ear (Li et al., 2005; Schlueter et al., 2007). In this study, we provide further evidence supporting the notion that zebrafish Igfbp3 has IGF-dependent actions. Our results showed that zebrafish Igfbp3 can bind to IGF ligands through its conserved IBD. When expressed in zebrafish embryos, the activities of the two mutants with impaired IGF binding ability (IBD mutant and IBD+NLS double mutant) were lower compared with that of the wild-type protein. Our in vivo experiments also demonstrated the IGF-independent action of Igfbp3 in zebrafish embryos. This is supported by the fact that the IBD mutant, which had little IGF binding activity, had significant dorsalizing activity in zebrafish embryos. Another line of evidence is that Igfbp3–EGFP, which had impaired IGF binding, had strong dorsalizing activity.

Mammalian IGFBP3 has been shown to possess distinct biological effects independently of IGF and IGF-1R (Firth and Baxter, 2002; Jogie-Brahim et al., 2009). There are several competing models regarding the molecular mechanisms underlying these IGF-independent actions of IGFBP3, including (1) interaction of IGFBP3 with its putative cell surface receptor; (2) nuclear localization and nuclear actions; (3) intracellular (but non-nuclear) action. Studies from a number of labs have shown that IGFBP3 has a functional NLS in its C-domain and is capable of nuclear translocation in cultured human tumor cells, and it can interact with retinoid-X receptor-α and other nuclear proteins in the nucleus (Liu et al., 2000; Oufattole et al., 2006). In addition, the N-domain of mammalian IGFBP3 has been shown to possess intrinsic transactivation activity (Zhao et al., 2006). Despite these findings, the in vivo significance of the nuclear localization and transactivation activity of IGFBP3 has not been explored. Our results show that the NLS mutant, which had impaired nuclear localization, and the transcription-dead TA mutant exhibited similar activity in dorsalizing the embryo to that seen with intact Igfbp3. These findings suggest that the dorsalizing effect of Igfbp3 is not dependent on its nuclear localization or transactivation activity in zebrafish embryos. These in vivo results in zebrafish are consistent with recent in vitro studies in human breast and prostate cancer cells, which show that the ability of IGFBP3 to inhibit cell growth and cause apoptosis does not require its nuclear localization (Butt et al., 2002). A more recent study reported that induction of apoptosis in human prostate cancer cells by IGFBP3 does not require binding to retinoid-X receptor-α either (Zappala et al., 2008). Taken together, these findings indicate that at least some of the ligand-independent actions of IGFBP3 are not related to its nuclear localization or transactivation activity. However, the high degree of structural and functional conservation of the NLS and TA uncovered by the current study, as well as previous reports on the functional interactions between nuclear IGFBP3 and several transcription factors suggest that these domains are functional. The nuclear actions of IGFBP3 might be dependent on the tissue, developmental stage and/or pathophysiological state.

A novel finding made in this study is that Igfbp3 exerts its ligand-binding-independent actions by antagonizing Bmp2 signaling (Fig. 9C). The Bmp signaling pathway has a crucial role in controlling the dorsal–ventral patterning in the zebrafish embryo (Schier and Talbot, 2005). Bmp signaling also regulates non-axial mesoderm patterning during gastrulation (Ramel et al., 2005) and is required for tail development in zebrafish (Agathon et al., 2003). As mentioned earlier, *swirl* and *somitabun*, two zebrafish genetic mutant lines caused by loss of function of *bmp2b* or *smad5*, exhibited the dorsalized phenotypes (Hild et al., 1999; Kishimoto et al., 1997). Forced expression of *bmp2b* in zebrafish embryos resulted in ventralized phenotypes (Kishimoto et al., 1997). In this study, we show that Igfbp3 antagonizes this action of Bmp2b. When co-expressed with Bmp2b in zebrafish embryos, Igfbp3 reduced Bmp2b-induced ventralization and abolished Bmp2b-induced *tp63* gene expression. Additionally, forced expression of Igfbp3 alone resulted in the dorsalized phenotypes, probably by blocking endogenous Bmp2 signaling. Importantly, the IBD mutant had similar effects. These results strongly suggest that zebrafish Igfbp3 can antagonize Bmp2 signaling in vivo, and this action is independent of IGF binding.

Many BMP antagonists, such as Chordin, Noggin and Follistatin, inhibit BMP signaling by forming a complex with a BMP ligand (Iemura et al., 1998; Piccolo et al., 1996; Zimmerman et al., 1996). Our biochemical data revealed that human IGFBP3 can also form a physical complex with BMP2. This interaction is specific to IGFBP3 because BMP2 did not bind to IGFBP1 or IGFBP6. Importantly, binding of IGFBP3 to BMP2 has functional significance because it inhibited BMP2-induced phosphorylation of Smad1/5/8 when tested in cultured human cells. In developing zebrafish embryos, *igfbp3* mRNA was first detected in the migrating neural crest cells and subsequently concentrated in pharyngeal arches and the inner ears (Li et al., 2005). *bmp2b* is widely expressed in early embryos, and becomes progressively restricted to the ventral half of the embryo by the onset of gastrulation (Kishimoto et al., 1997) and then expressed in otic vesicles (Martinez-Barbera et al., 1997) and pharyngeal endoderm (Thisse et al., 2004). Therefore, these two genes share overlapping domains, at least at some stage during embryogenesis. Moreover, both Bmp2 and Igfbp3 are secreted proteins and they can diffuse to surrounding tissues. Therefore, it is possible that they interact with each other in vivo.

Another interesting finding is that the expression of *chordin*, a well-known Bmp antagonist (Piccolo et al., 1996) that regulates dorsal development in zebrafish (Hammerschmidt et al., 1996), was upregulated in embryos injected with *igfbp3* mRNA. Because Bmp2 negatively regulates *chordin* gene expression at the transcriptional level (Zakin and De Robertis, 2010), the elevated *chordin* mRNA expression in Igfbp3-injected embryos is probably due to the binding and inhibition of Bmp2 signaling by zebrafish Igfbp3. Indeed, the results of co-injection experiments indicated that Bmp2b expression inhibited *chordin* gene expression in zebrafish embryos, and this action was attenuated by the co-expression of zebrafish Igfbp3. This action is independent of IGF because the IBD mutant had a similar effect. Further knockdown experiments indicate that Igfbp3 acts in a redundant manner to Chordin to antagonize Bmp2 in zebrafish embryos. Embryos injected with *chordin* MO and *igfbp3* MO showed more severe phenotypes with a greatly reduced head, expanded hematopoietic tissues and an enlarged tail compared with those injected with Chordin MO alone. A similar redundant relationship with Chordin has been reported for another BMP antagonist, Noggin, in zebrafish (Dal-Pra et al., 2006). This conclusion is further supported by overexpression studies, showing that Igfbp3 and Chordin had additive effects in antagonizing Bmp2. These results have led to a mechanistic model explaining the IGF-independent action of Igfbp3 in zebrafish embryos (Fig. 9C). According to the model, Igfbp3 binds to Bmp2 and possibly Bmp4 and inhibits its binding to its receptor and downstream Smad signaling activity. The reduced Bmp2 signaling leads to an increase in *chordin* gene expression as a result of the alleviation of the negative regulation of *chordin* gene expression by Bmp2. The increased Chordin in turn acts together with Igfbp3 to further antagonize Bmp2 activity. This results in the dorsalization of embryos.

The action of IGFBP3 in antagonizing BMP signaling appears to be evolutionarily conserved. This is supported by several lines of evidence: (1) human IGFBP3 and its IBD mutant had similar dorsalizing effects when expressed in zebrafish embryos; (2) human IGFBP3 inhibited human BMP2-induced Smad phosphorylation in cultured human U2OS cells in a dose-dependent manner; and (3) human IGFBP3 inhibited BMP2 action in 10T1/2 cell differentiation. BMPs belong to the TGFβ superfamily. Recent studies in a variety of mammalian cell cultures systems show that IGFBP3 can regulate cell growth and apoptosis by interacting with TGFβ at multiple levels (Fanayan et al., 2002; Fanayan et al., 2000; Forbes et al., 2010; Kuemmerle et al., 2004; Peters et al., 2006). In T47D breast cancer cells, the anti-growth action of IGFBP3 requires TGFβ receptor I/II and the downstream Smad2/3 (Fanayan et al., 2002; Fanayan et al., 2000). In human cytotrophoblasts, IGFBP3 was shown to affect basal proliferation via TGFβ receptor I/II and Smad2 (Forbes et al., 2010). Kuemmerle and co-workers (Kuemmerle et al., 2004) showed a direct binding of IGFBP3 to TGFβ receptor type II and V. A recent study (Mukherjee and Rotwein, 2008) reported that IGFBP5, the most closely related member of the IGFBP family, inhibited BMP-induced cell differentiation in an IGF-dependent manner. Although our data suggest that IGFBP3 can antagonize BMP signaling by binding to BMP2, other mechanisms might also be involved in the BMP-antagonizing action of IGFBP3.

Regulation of peptide growth factor by secreted binding proteins has emerged as a common theme in cell-to-cell signaling. Among the most extensively studied examples is IGFBP3. This multifunctional protein is involved in the regulation of cell proliferation, growth, migration, differentiation and apoptosis. The results of this study reveal that IGFBP3 acts in an IGF-dependent as well as an IGF-independent manner in a vertebrate animal model. Moreover, we discovered that IGFBP3 exerts IGF-independent actions by binding to and antagonizing BMP2 signaling. The results of this study provide new insights on the structural and functional conservation of the IGF binding, nuclear localization and transactivation domains of this multifunctional IGFBP. A better understanding of the molecular basis underlying the action of IGFBP3 will not only further our knowledge of IGFBP physiology but might also lead to future strategies for treating or circumventing human diseases.

Materials and Methods

Materials

Chemicals and reagents were purchased from Fisher Scientific (Pittsburgh, PA) unless noted otherwise. IGFs were purchased from GroPep (Adelaide, Australia) and IGFBPs and BMPs from R&D systems (Minneapolis, MN). Human Noggin was purchased from Neuromics (Edina, MN). Digoxigenin and anti-digoxigenin-POD antibody were purchased from Roche (Indianapolis, IN). Anti-GFP antibody was purchased from Torrey Pines Biolabs (East Orange, NJ). The anti- phosphorylated Smad1/5/8 antibody was purchased from Cell Signaling Technology (Danvers, MA)

and the total Smad1/5/8 antibody was purchased from Santa Cruz Biotechnology (Santa Cruz, CA). RNA polymerase and RNase-free DNase were purchased from Promega (Madison, WI). *Taq* DNA polymerase and endonucleases were purchased from New England BioLabs (Beverly, MA). *PfuUltra*™ II Fusion DNA Polymerase and STRATACLEAN™ Resin were purchased from Stratagene (LA Jolla, CA). M-MLV reverse transcriptase and oligonucleotide primers were purchased from Invitrogen Life Technologies (Carlsbad, CA).

Experimental animals

Wild-type zebrafish (*Danio rerio*) were maintained on a 14 hour light, 10 hour dark cycle and fed twice daily. Embryos were obtained by natural cross. Fertilized eggs were raised at 28.5°C and staged according to Kimmel and colleagues (Kimmel et al., 1995). 2-phenylthiourea [0.003% (w/v)] was added to the embryo rearing solution in some experiments to inhibit embryo pigment formation. All experiments were conducted in accordance with guidelines approved by the University Committee on the Use and Care of Animals at the University of Michigan.

Plasmid construction

The construction of the pCS2+Igfbp3 plasmid was reported (Li et al., 2005). The zebrafish Igfbp3 mutants were generated by site-directed mutagenesis using *PfuUltra*™ II Fusion DNA Polymerase. For the IBD mutant, K70, P71, L72, L75 and L76 were mutated to N, Q, Q, Q and Q. The NLS mutant was generated by mutating 236-KGRK-239 into LDGQ, the corresponding sequence of zebrafish Igfbp1a. The IBD+NLS double mutant was generated using the IBD mutant DNA as the template. The TA dead mutant was generated by changing E8, D11, D12 and E44 in zebrafish Igfbp3 into the corresponding residues of human IGFBP1. For cellular localization studies, DNA encoding Igfbp3 and its mutants were subcloned to the pCS2+EGFP vector. For this, the sense primer contains a *Bam*HI site followed by Kozak and the start of coding sequence: 5′-CGGGATCCGCCACCATGACAGGTCTGTGTGCGCTC-3′. The antisense primer contained an *Eco*RI site followed by the last seven amino acid coding sequence of zebrafish Igfbp3 without its stop codon: 5′-CGGAATTCGCTTTGTCTCCATG-TTATAGC-3′.

To generate Gal4DNA binding domain (DBD) and Igfbp3 fusion protein constructs, DNA fragments encoding zebrafish Igfbp3 N-domain or its TA mutant were amplified by PCR. The PCR products were cloned into the *Bam*HI-*Not*I sites of the pBind vector to fuse the Igfbp3 in-frame to the C-terminus of Gal4DBD.

Zebrafish *bmp2b* (GenBank: NM 131360) cDNA was cloned into the pCS2+ vector using the *Bam*HI and *Eco*RI sites. Human IGFBP3 and its IBD mutant were generated as previously reported (Imai et al., 2000). *tp63* (NM_152248) partial sequence used for the whole mount in situ hybridization was amplified. This sequence was subcloned into pGEM-T easy (Promega). Probe for *tp63* was linearized with *Nde*I and synthesized with T7.

Cell culture, transfection, and one-hybrid transcription activation assay

Human embryonic kidney (HEK) 293T cells, U2 osteosarcoma (U2OS) cells, and mouse C3H/10T1/2 clone 8 cells, purchased from American Type Culture Collection (Manassas, VA), were cultured according to ACTT's recommendation. To produce Igfbp3 and its mutant proteins, 2 μg pCS2+Igfbp3 and its mutant DNA were transfected into HEK293 cells, respectively. Conditioned media were prepared as reported previously (Duan et al., 1999). For one-hybrid assay, 500 ng pBind or pBind-IGFBP DNA and 500 ng pG5-luc DNA were co-transfected into cells as reported previously (Xu et al., 2004). 24 hours after transfection, cells were washed with PBS and lyzed in lysis buffer. Protein concentration was determined using a BCA protein assay kit (Pierce). Transcription activation was quantified using the Dual-Luciferase Reporter assay system (Promega). Firefly luciferase activity was divided by *Renilla* luciferase activity to normalize for transfection efficiency.

Western immunoblotting and ligand blotting and subcellular localization

Cell lysates or conditioned media from transfected cells were subjected to western blotting. IGFs, and BMPs were labeled with digoxingenin and used in ligand blotting following published methods (Shimizu et al., 2000). Subcellular localization studies were performed following published procedure (Xu et al., 2004).

Microinjection experiment

Capped mRNA synthesis was carried out using a commercial kit and linearized plasmid DNA as a template (mMESSAGE mMACHINE kit; Ambion). 1 nl Igfbp3 or its mutant mRNA was microinjected into 1- to 2-cell-stage zebrafish embryos (1 ng/embryo). For co-injection experiment, *bmp2b* mRNA (2.5 pg/embryo) was injected with or without *igfbp3* mRNA or mRNA encoding Igfbp3 with mutant IBD (1 ng/embryo); *chordin* mRNA (20 pg/embryos) was injected with or without *igfbp3* mRNA (500 pg/embryos). Embryos injected with *egfp* mRNA and intact embryos were used as controls. Previously validated morpholino-modified oligonucleotides (MOs) were used to knock down Igfbp3 (Li et al., 2005) and/or Chordin (Nasevicius and Ekker, 2000). The MO were dissolved in 1× Danieau Solution and injected into 1- to 2-cell-stage embryos, as reported previously (Li et al., 2005). A standard control MO was used as the control (Gene Tools, LLC, Philomath, OR). Embryos were injected with 4 ng control MO, 2 ng control MO plus 2 ng *chordin* MO, 2 ng *chordin* MO plus 2 ng *igfbp3* MO, or 2 ng control MO plus *igfbp3* MO, respectively. After microinjection, embryos were raised in embryo-rearing medium (Westerfield, 1995) and kept at 28.5°C. Live embryos were imaged.

Whole-mount in situ hybridization and qRT-PCR analysis

Whole-mount in situ hybridization was performed as reported previously (Maures and Duan, 2002). For qRT-PCR analysis, total RNA was extracted using TRIzol Reagent according to the manufacturer's instruction (Invitrogen Life Technologies, Carlsbad, CA). After DNase treatment, RNA (1 μg) was reverse-transcribed with random hexamer primers and M-MLV reverse transcriptase. qPCR was carried out in an iCycler iQ Multicolor real-time PCR detection system (Bio-Rad Laboratories, Hercules, CA) using SYBR® Premix Ex Taq™ (Takara Bio, Liaoning, China). Sequences of primers used for qPCR were: *tp63* (forward, 5′-AGAGAT-GGTCAGGTTTTGGG-3′; reverse, 5′-GTGCTGTTTGCGGATGC-3′); *chordin* (forward, 5′-ACGCCTGCTGCCATACAAT-3′; reverse, 5′-CACTGAGGGT-CCACCGAGA-3′); and β-actin (forward, 5′-AGAGTCCATCACGATACCAG-3′; reverse, 5′-AGAGTCCATCACGATACCAG-3′). Each sample was measured in duplicate. *tp63* and *chordin* mRNA levels were calculated using $2^{-\Delta\Delta Ct}$ method (Livak and Schmittgen, 2001) and presented as relative (fold) values of the control group after values were normalized to levels of β-actin.

In vitro BMP2 signaling activity

Human U2OS cells were seeded into 24-well plates. After 24 hours, the cells were washed and serum starved for 3 hours. 50 ng/ml human BMP2 were premixed and incubated with or without human IGFBP3 at various concentrations for 3 hours at room temperature. The premixed solution was added to the U2OS cells. 3 hours later, cells were harvested in RIPA buffer containing protease and phosphatase inhibitors (10 μg/ml aprotinin, 10 μg/ml leupeptin, 10 μg/ml pepstatin, 1 mM PMSF, 1 mM sodium orthovanadate, 1 mM sodium fluoride) and subjected to western immunoblotting.

Alkaline phosphatase (ALP) activity assay

The effects of human IGFBP3 and BMP2 on cell differentiation were examined in C3H/10T1/2 cells following the published method (Katagiri et al., 1990). ALP activity was measured using an Alkaline Phosphatase Assay kit (AnaSpec).

Statistical analysis

Values are presented as means ± s.d. Differences among groups were analyzed by one-way ANOVA followed by Tukey's Multiple Comparison Test or by unpaired *t* test using GraphPad Prism version 5.01 (San Diego, CA). Significance was accepted at $P<0.05$.

We thank Lisa Hebda and Catherine Nosal and John Allard, University of Michigan for proof reading this manuscript. We are grateful for A. C. Lekven, W. S. Talbot and H. Condamine for providing reagents. This study was supported by NSF Research Grant IOB 0110864, and Natural Scientific Foundation of China Grant 30928021, and the University Innovation Project Seed Grant 070742 from the Chinese Ministry of Education. Y.Z. is supported in part by a fellowship from China Scholarship Council.

Supplementary material available online at
http://jcs.biologists.org/cgi/content/full/124/11/1925/DC1

References

Agathon, A., Thisse, C. and Thisse, B. (2003). The molecular nature of the zebrafish tail organizer. *Nature* **424**, 448-452.

Bakkers, J., Hild, M., Kramer, C., Furutani-Seiki, M. and Hammerschmidt, M. (2002). Zebrafish DeltaNp63 is a direct target of Bmp signaling and encodes a transcriptional repressor blocking neural specification in the ventral ectoderm. *Dev. Cell* **2**, 617-627.

Buckway, C. K., Wilson, E. M., Ahlsen, M., Bang, P., Oh, Y. and Rosenfeld, R. G. (2001). Mutation of three critical amino acids of the N-terminal domain of IGF-binding protein-3 essential for high affinity IGF binding. *J. Clin. Endocrinol. Metab.* **86**, 4943-4950.

Butt, A. J., Fraley, K. A., Firth, S. M. and Baxter, R. C. (2002). IGF-binding protein-3-induced growth inhibition and apoptosis do not require cell surface binding and nuclear translocation in human breast cancer cells. *Endocrinology* **143**, 2693-2699.

Clemmons, D. R. (2007). Modifying IGF1 activity: an approach to treat endocrine disorders, atherosclerosis and cancer. *Nat. Rev. Drug Discov.* **6**, 821-833.

Dal-Pra, S., Furthauer, M., Van-Celst, J., Thisse, B. and Thisse, C. (2006). Noggin1 and Follistatin-like2 function redundantly to Chordin to antagonize BMP activity. *Dev. Biol.* **298**, 514-526.

Duan, C. and Xu, Q. (2005). Roles of insulin-like growth factor (IGF) binding proteins in regulating IGF actions. *Gen. Comp. Endocrinol.* **142**, 44-52.

Duan, C., Ding, J., Li, Q., Tsai, W. and Pozios, K. (1999). Insulin-like growth factor binding protein 2 is a growth inhibitory protein conserved in zebrafish. *Proc. Natl. Acad. Sci. USA* **96**, 15274-15279.

Fanayan, S., Firth, S. M., Butt, A. J. and Baxter, R. C. (2000). Growth inhibition by insulin-like growth factor-binding protein-3 in T47D breast cancer cells requires

transforming growth factor-beta (TGF-beta) and the type II TGF-beta receptor. *J. Biol. Chem.* **275**, 39146-39151.

Fanayan, S., Firth, S. M. and Baxter, R. C. (2002). Signaling through the Smad pathway by insulin-like growth factor-binding protein-3 in breast cancer cells. Relationship to transforming growth factor-beta 1 signaling. *J. Biol. Chem.* **277**, 7255-7261.

Firth, S. M. and Baxter, R. C. (2002). Cellular actions of the insulin-like growth factor binding proteins. *Endocr. Rev.* **23**, 824-854.

Forbes, K., Souquet, B., Garside, R., Aplin, J. D. and Westwood, M. (2010). Transforming growth factor-{beta} (TGF{beta}) receptors I/II differentially regulate TGF{beta}1 and IGF-binding protein-3 mitogenic effects in the human placenta. *Endocrinology* **151**, 1723-1731.

Hammerschmidt, M., Pelegri, F., Mullins, M. C., Kane, D. A., van Eeden, F. J., Granato, M., Brand, M., Furutani-Seiki, M., Haffter, P., Heisenberg, C. P. et al. (1996). dino and mercedes, two genes regulating dorsal development in the zebrafish embryo. *Development* **123**, 95-102.

Hild, M., Dick, A., Rauch, G. J., Meier, A., Bouwmeester, T., Haffter, P. and Hammerschmidt, M. (1999). The smad5 mutation somitabun blocks Bmp2b signaling during early dorsoventral patterning of the zebrafish embryo. *Development* **126**, 2149-2159.

Hong, J., Zhang, G., Dong, F. and Rechler, M. M. (2002). Insulin-like growth factor (IGF)-binding protein-3 mutants that do not bind IGF-I or IGF-II stimulate apoptosis in human prostate cancer cells. *J. Biol. Chem.* **277**, 10489-10497.

Iemura, S., Yamamoto, T. S., Takagi, C., Uchiyama, H., Natsume, T., Shimasaki, S., Sugino, H. and Ueno, N. (1998). Direct binding of follistatin to a complex of bone-morphogenetic protein and its receptor inhibits ventral and epidermal cell fates in early Xenopus embryo. *Proc. Natl. Acad. Sci. USA* **95**, 9337-9342.

Imai, Y., Moralez, A., Andag, U., Clarke, J. B., Busby, W. H., Jr and Clemmons, D. R. (2000). Substitutions for hydrophobic amino acids in the N-terminal domains of IGFBP-3 and -5 markedly reduce IGF-I binding and alter their biologic actions. *J. Biol. Chem.* **275**, 18188-18194.

Jogie-Brahim, S., Feldman, D. and Oh, Y. (2009). Unraveling insulin-like growth factor binding protein-3 actions in human disease. *Endocr. Rev.* **30**, 417-437.

Joly, J. S., Joly, C., Schulte-Merker, S., Boulekbache, H. and Condamine, H. (1993). The ventral and posterior expression of the zebrafish homeobox gene eve1 is perturbed in dorsalized and mutant embryos. *Development* **119**, 1261-1275.

Katagiri, T., Yamaguchi, A., Ikeda, T., Yoshiki, S., Wozney, J. M., Rosen, V., Wang, E. A., Tanaka, H., Omura, S. and Suda, T. (1990). The non-osteogenic mouse pluripotent cell line, C3H10T1/2, is induced to differentiate into osteoblastic cells by recombinant human bone morphogenetic protein-2. *Biochem. Biophys. Res. Commun.* **172**, 295-299.

Kimmel, C. B., Ballard, W. W., Kimmel, S. R., Ullmann, B. and Schilling, T. F. (1995). Stages of embryonic development of the zebrafish. *Dev. Dyn.* **203**, 253-310.

Kishimoto, Y., Lee, K. H., Zon, L., Hammerschmidt, M. and Schulte-Merker, S. (1997). The molecular nature of zebrafish swirl: BMP2 function is essential during early dorsoventral patterning. *Development* **124**, 4457-4466.

Kuemmerle, J. F., Murthy, K. S. and Bowers, J. G. (2004). IGFBP-3 activates TGF-beta receptors and directly inhibits growth in human intestinal smooth muscle cells. *Am. J. Physiol. Gastrointest. Liver Physiol.* **287**, G795-G802.

Li, Y., Xiang, J. and Duan, C. (2005). Insulin-like growth factor-binding protein-3 plays an important role in regulating pharyngeal skeleton and inner ear formation and differentiation. *J. Biol. Chem.* **280**, 3613-3620.

Liu, B., Lee, H. Y., Weinzimer, S. A., Powell, D. R., Clifford, J. L., Kurie, J. M. and Cohen, P. (2000). Direct functional interactions between insulin-like growth factor-binding protein-3 and retinoid X receptor-alpha regulate transcriptional signaling and apoptosis. *J. Biol. Chem.* **275**, 33607-33613.

Livak, K. J. and Schmittgen, T. D. (2001). Analysis of relative gene expression data using real-time quantitative PCR and the 2(-Delta Delta C(T)) method. *Methods* **25**, 402-408.

Martinez-Barbera, J. P., Toresson, H., Da Rocha, S. and Krauss, S. (1997). Cloning and expression of three members of the zebrafish Bmp family: Bmp2a, Bmp2b and Bmp4. *Gene* **198**, 53-59.

Maures, T. J. and Duan, C. (2002). Structure, developmental expression, and physiological regulation of zebrafish IGF binding protein-1. *Endocrinology* **143**, 2722-2731.

Miller-Bertoglio, V. E., Fisher, S., Sanchez, A., Mullins, M. C. and Halpern, M. E. (1997). Differential regulation of chordin expression domains in mutant zebrafish. *Dev. Biol.* **192**, 537-550.

Mukherjee, A. and Rotwein, P. (2008). Insulin-like growth factor-binding protein-5 inhibits osteoblast differentiation and skeletal growth by blocking insulin-like growth factor actions. *Mol. Endocrinol.* **22**, 1238-1250.

Nasevicius, A. and Ekker, S. C. (2000). Effective targeted gene 'knockdown' in zebrafish. *Nat. Genet.* **26**, 216-220.

Nikaido, M., Kawakami, A., Sawada, A., Furutani-Seiki, M., Takeda, H. and Araki, K. (2002). Tbx24, encoding a T-box protein, is mutated in the zebrafish somite-segmentation mutant fused somites. *Nat. Genet.* **31**, 195-199.

Oufattole, M., Lin, S. W., Liu, B., Mascarenhas, D., Cohen, P. and Rodgers, B. D. (2006). Ribonucleic acid polymerase II binding subunit 3 (Rpb3), a potential nuclear target of insulin-like growth factor binding protein-3. *Endocrinology* **147**, 2138-2146.

Peters, I., Tossidou, I., Achenbach, J., Woroniecki, R., Mengel, M., Park, J. K., Paschy, M., de Groot, K., Haller, H. and Schiffer, M. (2006). IGF-binding protein-3 modulates TGF-beta/BMP-signaling in glomerular podocytes. *J. Am. Soc. Nephrol.* **17**, 1644-1656.

Piccolo, S., Sasai, Y., Lu, B. and De Robertis, E. M. (1996). Dorsoventral patterning in Xenopus: inhibition of ventral signals by direct binding of chordin to BMP-4. *Cell* **86**, 589-598.

Radulescu, R. T. (1995). From insulin, retinoblastoma protein and the insulin receptor to a new model on growth factor specificity: the nucleocrine pathway. *J. Endocrinol.* **146**, 365-368.

Ramel, M. C., Buckles, G. R., Baker, K. D. and Lekven, A. C. (2005). WNT8 and BMP2B co-regulate non-axial mesoderm patterning during zebrafish gastrulation. *Dev. Biol.* **287**, 237-248.

Schedlich, L. J., Young, T. F., Firth, S. M. and Baxter, R. C. (1998). Insulin-like growth factor-binding protein (IGFBP)-3 and IGFBP-5 share a common nuclear transport pathway in T47D human breast carcinoma cells. *J. Biol. Chem.* **273**, 18347-18352.

Schier, A. F. and Talbot, W. S. (2005). Molecular genetics of axis formation in zebrafish. *Annu. Rev. Genet.* **39**, 561-613.

Schlueter, P. J., Peng, G., Westerfield, M. and Duan, C. (2007). Insulin-like growth factor signaling regulates zebrafish embryonic growth and development by promoting cell survival and cell cycle progression. *Cell Death Differ.* **14**, 1095-1105.

Shimizu, M., Swanson, P., Fukada, H., Hara, A. and Dickhoff, W. W. (2000). Comparison of extraction methods and assay validation for salmon insulin-like growth factor-I using commercially available components. *Gen. Comp. Endocrinol.* **119**, 26-36.

Shimizu, T., Yamanaka, Y., Nojima, H., Yabe, T., Hibi, M. and Hirano, T. (2002). A novel repressor-type homeobox gene, ved, is involved in dharma/bozozok-mediated dorsal organizer formation in zebrafish. *Mech. Dev.* **118**, 125-138.

Talbot, W. S., Trevarrow, B., Halpern, M. E., Melby, A. E., Farr, G., Postlethwait, J. H., Jowett, T., Kimmel, C. B. and Kimelman, D. (1995). A homeobox gene essential for zebrafish notochord development. *Nature* **378**, 150-157.

Thisse, B., Heyer, V., Lux, A., Alunni, V., Degrave, A., Seiliez, I., Kirchner, J., Parkhill, J. P., and Thisse, C. (2004). Spatial and temporal expression of the zebrafish genome by large-scale in situ hybridization screening. *Methods Cell Biol.* **77**, 505-519.

Westerfield, M. (1995). *The Zebrafish Book*. Eugene, OR: University of Oregon Press.

Xu, Q., Li, S., Zhao, Y., Maures, T. J., Yin, P. and Duan, C. (2004). Evidence that IGF binding protein-5 functions as a ligand-independent transcriptional regulator in vascular smooth muscle cells. *Circ. Res.* **94**, E46-E54.

Yamada, P. M. and Lee, K. W. (2009). Perspectives in mammalian IGFBP-3 biology: local vs. systemic action. *Am. J. Physiol. Cell Physiol.* **296**, C954-C976.

Zakin, L. and De Robertis, E. M. (2010). Extracellular regulation of BMP signaling. *Curr. Biol.* **20**, R89-R92.

Zappala, G., Elbi, C., Edwards, J., Gorenstein, J., Rechler, M. M. and Bhattacharyya, N. (2008). Induction of apoptosis in human prostate cancer cells by insulin-like growth factor binding protein-3 does not require binding to retinoid X receptor-alpha. *Endocrinology* **149**, 1802-1812.

Zhao, Y., Yin, P., Bach, L. A. and Duan, C. (2006). Several acidic amino acids in the N-domain of insulin-like growth factor-binding protein-5 are important for its transactivation activity. *J. Biol. Chem.* **281**, 14184-14191.

Zimmerman, L. B., De Jesus-Escobar, J. M. and Harland, R. M. (1996). The Spemann organizer signal noggin binds and inactivates bone morphogenetic protein 4. *Cell* **86**, 599-606.